The structural design of the bat wing web and its possible role in gas exchange

Andrew N. Makanya[1] and Jacopo P. Mortola[2]

[1]*Department of Veterinary Anatomy & Physiology, University of Nairobi, Kenya*
[2]*Department of Physiology, McGill University, Montreal, Quebec, Canada*

Abstract

The structure of the skin in the epauletted fruit bat (*Epomophorus wahlbergi*) wing and body trunk was studied with a view to understanding possible adaptations for gas metabolism and thermoregulation. In addition, gas exchange measurements were performed using a respirometer designed for the purpose. The body skin had an epidermis, a dermis with hair follicles and sweat glands and a fat-laden hypodermis. In contrast, the wing web skin was made up of a thin bilayered epidermis separated by a connective tissue core with collagen and elastic fibres and was devoid of hair follicles and sweat glands. The wings spanned 18–24 cm each, with about 753 cm^2 of surface exposed to air. The body skin epidermis was thick (61 ± 3 μm, SEM), the stratum corneum alone taking a third of it (21 ± 3 μm). In contrast, the wing web skin epidermis was thinner at 9.8 ± 0.7 μm, with a stratum corneum measuring 4.1 ± 0.3 μm (41%). The wing capillaries in the wing web skin ran in the middle of the connective tissue core, with a resultant surface-capillary diffusion distance of 26.8 ± 3.2 μm. The rate of oxygen consumption ($\dot{V}O_2$) of the wings alone and of the whole animal measured under light anaesthesia at ambient temperatures of 24 °C and 33 °C, averaged 6% and 10% of the total, respectively. Rate of carbon dioxide production had similar values. The membrane diffusing capacity for the wing web was estimated to be 0.019 ml O_2 min^{-1} mmHg^{-1}. We conclude that in *Epomophorus wahlbergi*, the wing web has structural modifications that permit a substantial contribution to the total gas exchange.
Key words bat; morphometry; skin gas exchange; wing web structure.

Introduction

Volancy is an elegant, albeit energetically expensive form of locomotion. In the evolution of vertebrate flight the forelimb was modified for aerial locomotion, with the consequence that it became elongated and the flight muscles were shifted close to the body's centre of gravity to minimize the weight of the wings (Neuweiler, 2000). With respect to cost per unit distance covered, powered flight is a very efficient mode of transport (Schmidt-Nielsen, 1972). Birds and bats are the only extant vertebrate taxa that have achieved active flight. This elite mode of locomotion was achieved by employing diverse adaptive schemes and strategies (Maina, 2000; Sears et al. 2006), which necessitated certain trade-offs and compromises. Bats modified a fundamentally mammalian lung and combined this with diverse physiological refinements to obtain the large amounts of oxygen required for flight (Maina, 2000). In birds, an ancestral reptilian organ was modified to the lung–air sac system characteristic of the extant avian species (Duncker, 1972; Duncker & Guentert, 1985).

Notably, powered flight evolved in only three taxa: the insects, bats and birds (Maina, 2000). The wing appears to be a fundamental structure in active flight and thus it is encountered in all the three taxa capable of this graceful mode of locomotion. In bats, the forelimb was modified into a wing with elongate finger bones joined together by a thin membrane (Thewissen & Babcock, 1992). The bat wing surface area is high at about 85% of the total body surface area (Baker, 1966, cited by Bassett & Studier, 1988), and has a rich blood perfusion. Consequently, bat wings participate in heat and water control (Kluger & Heath, 1970; Bakken & Kunz, 1988; Bassett & Studier, 1988; Thomspon & Speakman, 1999). Gas exchange via the skin requires diffusion of O_2 and CO_2 between the environment and the subcutaneous vessels, through the skin layers. In most mammals this mechanism contributes only a minuscule fraction of total gas exchange, as mammals have high metabolic needs and their body surface-to-volume ratio is too small for the skin to supply a significant proportion of the necessary gas exchange requirements. Furthermore, the thickness of the skin layers and the establishment of the epidermal barrier (Cartlidge, 2000), while limiting water loss, greatly hinder the diffusion rate of the respiratory gases. In mammals, the skin is an important route for gas

Correspondence

Andrew N. Makanya, PhD, Department of Veterinary Anatomy & Physiology, University of Nairobi, Riverside Drive, Chiromo Campus, P.O. Box 30197-00100, Nairobi, Kenya. T: +254 20 444 6764; F: +254 20 445 1770; E: makanya@uonbi.ac.ke

exchange only in some newborn marsupials with body weights of about 300 mg or less (Mortola et al. 1999; MacFarlane & Frappell, 2001). In these neonates, the large body surface-to-volume ratio, the plausibly thin skin and the low metabolic requirements combine in making the skin the primary gas exchange organ.

Notably, the bat wing has its two surfaces exposed to the environment during flight, thus enormously increasing the skin surface potentially available for gas diffusion. In addition, the wing web vessels are capable of adjusting blood flow to various stimuli (Wiegman et al. 1975; Harris et al. 1976; Davis, 1988a,b). Herreid et al. (1968) measured the CO_2 eliminated by the wings of conscious and immobilized bats, and compared it to the published values of the total rate of oxygen consumption ($\dot{V}O_2$), assuming a Respiratory Quotient of 0.8. From this computation, the contribution of the wing to $\dot{V}O_2$ was estimated to be as high as 11.5% of the total.

In the current study, we compare the structural characteristics of the wing web skin with the body skin, to examine the morphological basis for gas exchange. In addition we have simultaneously measured the $\dot{V}O_2$ and $\dot{V}CO_2$ of the wing and of the whole animal, in cold and warm conditions. The results indicate that the wing web can provide a substantial contribution to the overall gas exchange in bats.

Materials and methods

Experimental animals

Experiments were conducted on adult epauletted fruit bats *Epomophorus wahlbergi* (Acharya, 1992). The experimental animals were obtained from the Department of Mammalogy, National Museums of Kenya. The animals were trapped locally by mist netting and maintained in cages at ambient temperatures of 21 °C, with water and fruits (bananas, mangos) *ad libitum*. The bats were allowed to acclimatize to the laboratory conditions for 1 day before any measurements were taken. The aforementioned institution had the appropriate permits for capture of bats.

Measurements of gaseous metabolism

Measurements of $\dot{V}O_2$ and $\dot{V}CO_2$ were performed on five bats, using an open-loop methodology (Frappell et al. 1992). The set-up is schematically depicted in Fig. 1. The animals (four males, one female, average body weight 98 g, range 68–125 g) were given mild anaesthesia with a mixture of ketamine (3 mg kg^{-1}) and xylazine (15 mg kg^{-1}) applied intramuscularly. This combination of anaesthetics was recommended for chiroptera (Pye, 2001) as it has a rapid action with gradual and uneventful recovery. By the end of the measurements, 3–4 h after the onset of anaesthesia, all animals were beginning to respond to stimuli, and, shortly after, were freely moving. Body weight was measured on a scale accurate to 10^{-2} g. The surface area of the distended wing was measured in three anaesthetized bats by tracing the silhouette, and calculating the area with a digitizing tablet connected to a microcomputer.

To measure pulmonary and cutaneous gas exchange, the bat under study was suspended head down, gripping a long stick placed horizontally across the top compartment of a double-chamber plastic respirometer (Fig. 1). The central portion of the chamber separator was made of a double layer of a soft polyethylene plastic sheet, with a hole at the centre. The head of the bat fitted through this hole and the plastic membrane fitted around the neck,
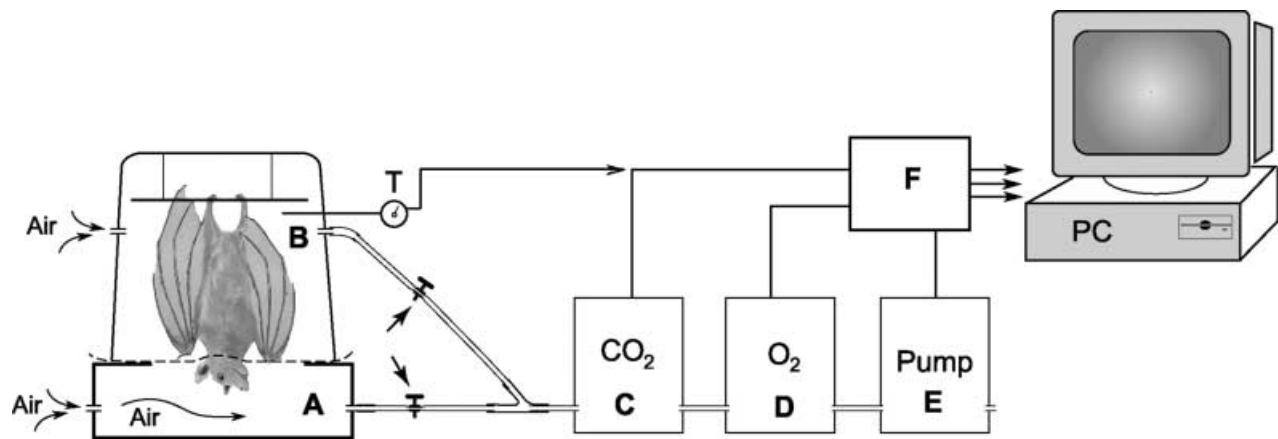

Fig. 1 Schematic diagram showing the set-up of the equipment used for the measurements of rates of oxygen consumption and carbon dioxide production in the bat. A thin polyethylene separator was fitted around the animal's neck, dividing the respirometer into a lower compartment (A) which housed the head and an upper compartment (B), which housed the rest of the body of the animal. The gases flowing out of the chambers were dried and channeled by a pump through a carbon dioxide analyser and an oxygen analyser for measurements of the concentration of the respective gases. The outputs of the analysers, with the pump flow and the respirometer temperature, were conveyed to an Analog Digital Data Conversion Board for on-line display, acquisition and data analysis by a mini-computer (PC). Analysis of the gases from either of the compartments could be accomplished by opening the respective valves. Further details are provided under Materials and methods.

providing an adequate seal that completely separated the lower chamber from the upper one. Hence, the head was housed in the lower chamber, while the rest of the body was in the upper chamber. No attempts were made to distend the wings, which were in the folded position normally observed during roosting. The ambient temperature in the respirometer was monitored with a tungsten-constantan thermocouple (DP30, Omega, Laval, Quebec, Canada) and could be varied by adjusting the distance of a heating infrared lamp, which was placed external to the chamber. Each compartment of the respirometer had anterior and posterior openings. The posterior openings were for the entrance of air, and the anterior ones were connected to a common final pathway via polyethylene tubing, which could be clamped to isolate one compartment from the other. A mini-pump with built-in mass flow meter (TR-SS3, Sable Systems, Las Vegas, NV, USA) maintained a constant gas flow of 300 mL min^{-1} through the upper and lower compartments, either in combination or individually. The gas passed through a drying column, and was analysed for O_2 and CO_2 concentration by a fuel cell O_2 analyser and an infrared CO_2 analyser (respectively, FoxBox and CA10A, Sable Systems), arranged in series. The outputs of the analysers, together with those of the pump and the respirometer temperature, were displayed on a computer monitor during on-line acquisition. Values for $\dot{V}O_2$ and $\dot{V}CO_2$ were computed from the flow rate and the inflow–outflow gas concentration difference.

After at least 30 min from the onset of anaesthesia, measurements were collected by alternating sampling periods of 15–30 min each, either from both compartments combined, yielding the total $\dot{V}O_2$ and $\dot{V}CO_2$, or from the upper compartment in isolation, yielding the $\dot{V}O_2$ and $\dot{V}CO_2$ for the wings. Measurements of total and wing $\dot{V}O_2$ and $\dot{V}CO_2$ were performed in an alternating order, and the runs repeated at two ambient temperatures, within the warm (32–36 °C) and cold (20–24 °C) range.

Skin morphology and morphometry

Macroscopic measurements to estimate wingspan and wing surface area were made on three bats. Morphological and morphometric details of the body and wing web skins were obtained from two bats, killed with an overdose of inhalant diethyl ether or intrabdominal injection of sodium pentobarbitone (Euthatal®, Merial Animal Health Ltd, Essex, UK). Skin strips were obtained randomly from the body trunk and boneless parts of the wing web. The skin strips were fixed by total immersion in a solution of 2.5% glutaraldehyde in 0.1 M cacodylate buffer (pH 7.4, 350 mOsm) and then cut into small tissue blocks. The tissue blocks were postfixed in osmium tetroxide, blockstained using uranyl acetate, dehydrated through ascending concentrations of ethanol starting with 70%, through 80%,

90%, two changes of 100%, and then embedded in epoxy resin. Tissue blocks were trimmed and semithin sections were obtained at 1 micron, stained with toluidine blue and viewed under a Leitz DMR Leica microscope (Mel Sobel Microscopes Ltd, Hicksville, NY, USA) equipped with a JVC KY-F70 digital camera.

After obtaining semithin sections, tissue blocks were further trimmed and ultrathin sections obtained at 90 nm, counterstained with lead citrate and viewed on a Philips EM-300 microscope (Carl-Zeiss, Oberkochen, Germany). For the scanning electron microscopy, tissue samples were fixed as described above, dehydrated in ascending concentrations of ethanol, critical point-dried in liquid carbon dioxide and subsequently sputter-coated with gold. The specimens were mounted on brass stubs and viewed on a Philips XL30 FEG scanning electron microscope.

Morphometric measurements were performed to estimate the thickness of the various components of the body and wing web skins. These included the entire epidermis, the keratinized layer (stratum corneum), the dermis and the hypodermis. The wing web did not have a distinct dermis or hypodermis; hence, the layer below the epidermis was measured as a single entity (dermis-hypodermis). The thickness of the wing skin was computed as an average of the thickness values of the boneless membrane measured perpendicular to the epidermal surface and then divided by two. Cutaneous diffusion distances were obtained as the distance from the epidermal surface to the inner surface of the core capillary endothelium. Measurements were done using ANALYSIS® imaging software (Version 3.2, Soft Imaging System, GmbH, Münster, Germany).

Wing membrane diffusing capacity

The membrane diffusing capacity (DMO_2) as exemplified in Weibel et al. (1993) is estimated from the formula:

$$DMO_2 = Kb * Sb * 1/\tau hb$$

where Kb is the Krogh's diffusion constant of the tissue barrier, assumed to be $3.3 * 10^{-8}$ cm^2 min^{-1} mmHg^{-1}; Sb is the diffusion surface area and τhb is the barrier thickness. The entire surface area of both sides of the wing was taken to be the diffusion surface and the barrier thickness was the measured diffusion distance from the epidermal surface to the inner surface of the wing membrane capillaries.

STATISTICAL ANALYSIS

Data were presented as group means ± SEM. For statistical comparisons, the two-tailed t-test was used, either unpaired (morphometric measurements of wing web vs. body skin), or paired (wing–total ratios for $\dot{V}O_2$ and $\dot{V}CO_2$ between warm and cold temperatures). In all cases, $P < 0.05$ defined the level of statistically significant difference.
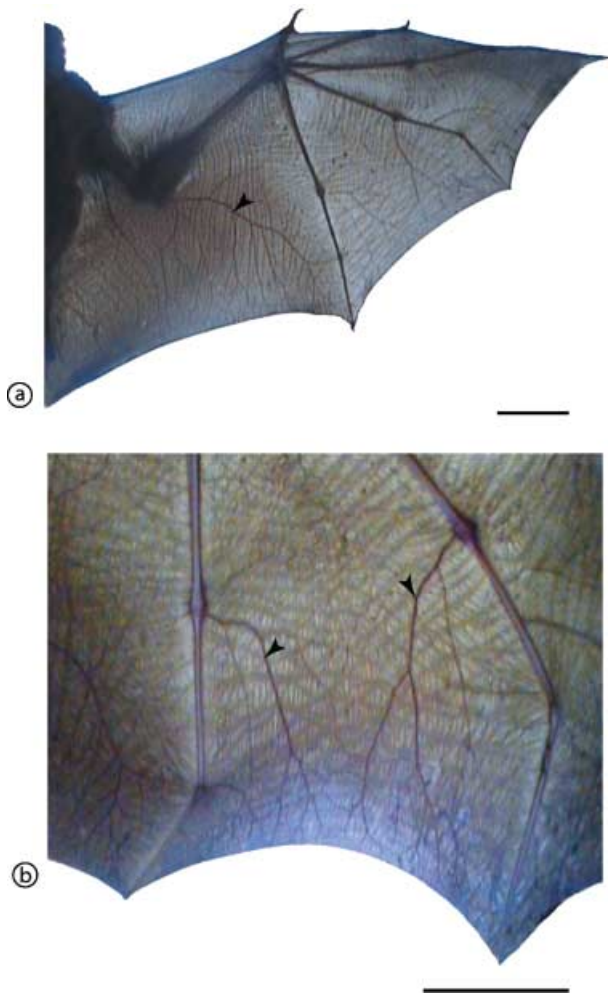
Fig. 2 Distribution of blood vessels in the bat wing web. (a) The whole wing, showing the distribution of the finger bones and large vessels (arrowhead) in the boneless wing membrane. Scale bar = 5 cm. (b) A higher magnification of the wing web membrane stretched between the fourth and fifth fingers with prominent large blood vessels. Scale bar = 5 cm. Notice the rich supply of blood vessels in the wing web.

Results

Macroscopic view

At the macroscopic level, the distended bat wing showed an intricate network of vessels filling the web space between the finger bones (Fig. 2). Unlike the body skin, the wing skin lacked hairs on either surface. In three bats (female of 72 g, male of 125 g and male of 111 g), the wing length (shoulder to tip) and the surface area of the silhouette of the extended wing were measured. The wing lengths were, respectively, 18, 24 and 19 cm (measurement for either of the two wings), and the respective total exposed surface areas of the two combined wings for each bat were 600, 1008, and 652 cm^2.

Table 1 Morphometric measurements of the thickness of the various skin layers in the bat body skin and the wing web skin. The membrane diffusing capacity for the wing web (DMO$_2$) is also presented

| Component	Region		
	Body skin	Wing web skin	P-value
Epidermis	60.6 ± 2.6	9.8 ± 0.7	< 0.001
Stratum corneum	20.6 ± 2.7	4.1 ± 0.3	< 0.001
Dermis	45.4 ± 7.1	–	–
Hypodermis	246.6 ± 12.6	–	–
Dermis–hypodermis	287.8 ± 15.0	15.5 ± 2.7	< 0.001
Diffusion distance	–	26.8 ± 3.3	–
Entire skin	329.6 ± 84.1	27.8 ± 3.1	< 0.001
DMO$_2$	–	0.019	

Values (in microns, except for DMO$_2$ which is in ml O$_2$ min^{-1} mmHg^{-1}) are means (± 1 SEM) of 11 determinations from two bats. The wing web skin did not have a distinct dermis or hypodermis; the two layers were combined into a single measurement. Diffusion distance and diffusion capacity were not determined for the body skin.

Light microscopy and morphometry

The structural differences between the wing web skin (WWS) and body skin (BS) were remarkable (Fig. 2). The wing web skin was highly folded (Fig. 2a,c) and lacked hair follicles. It comprised two epidermal layers separated by a central core of connective tissue. The blood vessels were located in the middle of the connective tissue core. Under the epidermis, there was no clear distinction between the dermis and the hypodermis. In contrast, the body skin was thick, had prominent hairs and hair follicles, a thick dermis and a hypodermis (Fig. 2b,d). In addition, the dermis of the body skin had prominent sweat glands, which were notably absent in the wing web.

The morphometric details on the BS and WWS are provided in Table 1. The entire BS had a thickness of 329.6 ± 84.1 μm, with an epidermis of 61 ± 3 μm. The stratum corneum of the BS alone took a third of the epidermis at 21 ± 3 μm. In contrast, the WWS was thinner at 27.8 ± 3.1 μm, but the epidermis made up a larger proportion of the thickness at 9.8 ± 0.7 μm. The stratum corneum in the WWS was 4.1 ± 0.3 μm thick. Diffusion distances (i.e. distance from skin surface to the inner surface of the capillary endothelium) averaged 26.8 ± 3.3 μm. The thickness of all the skin layers was significantly smaller in the wing web than in the body skin (Table 1). The thickness of dermis and hypodermis combined in the wing web was only 5.4% of that of the corresponding layers in the body skin. Indeed, the epidermis in the body skin alone was thicker than all the layers of the wing web combined. Estimation of DMO$_2$ based on the measured wing area and the diffusion distances resulted in a value of 0.019 ml O$_2$ min^{-1} mmHg^{-1} (Table 1).

Fig. 3 Semithin sections comparing the structural characteristics of the wing web skin (left panels) and body skin (right panels) in the bat. (a,b) Low magnification (scale bars = 500 μm). Note the enormous folding of the wing web skin compared to the body skin. Hair follicles (encircled) are evident in the body skin. (c,d) Intermediate magnification (scale bars = 100 μm). The wing web is highly folded, with a double layer of epidermis (rectangles in c). The demarcation between the epidermis and dermis is not evident and the two epidermal layers are separated by a central core of connective tissue (asterisks). Unlike the wing web skin, the body skin has a relatively thick epidermis (E), a conspicuous dermis (D) with prominent sweat glands (S) and hair follicles (arrowhead). Note also the hypodermis (H). (e,f) High magnification (scale bars = 10 μm). In the wing web, the thin epidermis (rectangle) is only a few cells thick, and the connective tissue core (asterisks) presents a central capillary network (arrowheads). At the same magnification, in the body skin only the epidermis (E) with a thick stratum corneum (asterisk) and part of the epidermis (D) with sweat glands (S) have been captured.
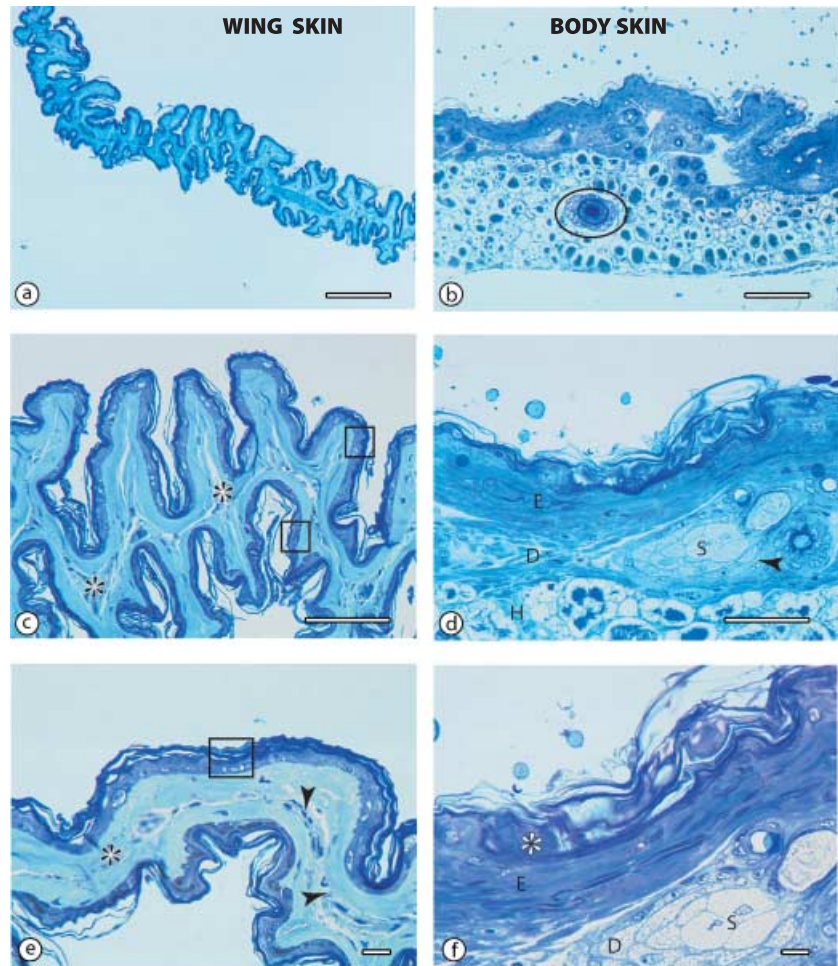
Scanning and transmission electron microscopy

Under the scanning electron microscope (Fig. 3) it was evident that the wing web skin was virtually devoid of hairs. Its rough surface presented keratinized layers in the process of peeling off (see also Figs 2 and 4). By contrast, a dense coat of long hairs, fully masking the skin surface, covered the body skin. Ultrastructural morphology revealed the fine details of the wing web (Fig. 5). The capillary layer was in the middle of the core tissue, approximately equidistant from both surfaces. Melanocytes were present in the core tissue and had many melanin granules. The non-keratinized part of the epidermis was about two cells thick, while the stratum corneum had up to 10 layers of relatively thin, squamous keratinocytes. Both the epidermal cells and the keratinocytes contained melanin granules, whereas the core tissue was made up mainly of elastic and collagen fibres.

Gaseous metabolism: total and wings

The values (individual and means) of $\dot{V}O_2$ and $\dot{V}CO_2$ are presented in Fig. 6. Rate of oxygen consumption for the whole body averaged 2.6 ± 0.3 and 2.2 ± 0.3 mL/min at the lower (24 ± 1 °C) and higher (33 ± 1 °C) temperatures, respectively. In the majority of bats $\dot{V}O_2$ was higher at the lower temperature, but the reverse pattern occurred in one bat (unfilled circle in Fig. 6). Qualitatively similar results were obtained for $\dot{V}CO_2$ (right panel in Fig. 6). The $\dot{V}O_2$ of the wings averaged 0.13 ± 0.02 and 0.21 ± 0.04 mL min^{-1} at the lower and higher temperatures, respectively. The corresponding values for $\dot{V}CO_2$ were 0.14 ± 0.02 and 0.20 ± 0.03 mL min^{-1}. These seemingly large differences between the two temperatures were, however, not statistically significant; in fact they were largely consequent to the behaviour of one animal, which showed a major increase in cutaneous gas exchange at the higher temperature (unfilled rhomboids in Fig. 6). On average, at the lower temperatures the wings provided $5.5 \pm 1.2\%$ of the total $\dot{V}O_2$ (range among animals: 1.9–9.2%) and $5.9 \pm 1.1\%$ of the total $\dot{V}CO_2$ (range among animals: 2.4–9.3%) (Fig. 7). At the higher temperatures, the values were $10.0 \pm 1.8\%$ for $\dot{V}O_2$ (range: 5.2–13.2%) and $10.0 \pm 1.6\%$ for $\dot{V}CO_2$ (range: 5.4–13.5%). In all animals the contribution of the wings to the total gas exchange was higher at the higher temperatures ($P < 0.01$).
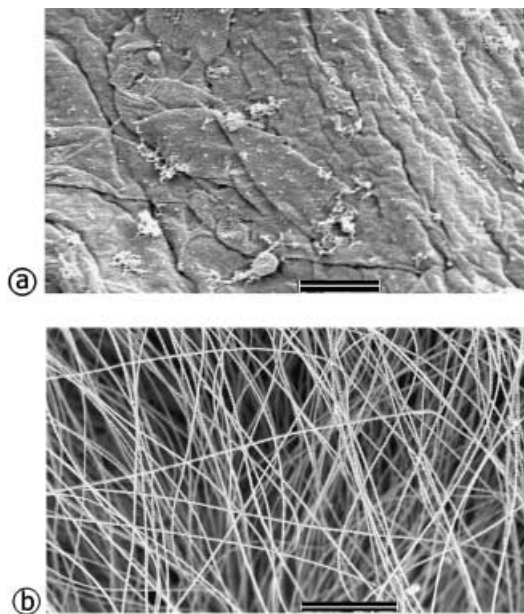
Fig. 4 Scanning electron micrographs of the wing web skin (a) and the body skin (b) showing the remarkable topographical differences. The wing web is virtually devoid of hairs. Its rough surface presents keratinized layers in the process of peeling off (see also Figs 3 and 5). In contrast, the body skin is virtually covered by a thick coat of tall hairs, fully masking the skin surface. Scale bars: a = 10 μm; b = 500 μm.

Discussion

As a form of locomotion, active flight is energetically very expensive, but energetically efficient as more distance is covered per unit of energy expended (Carpenter, 1975; Thomas, 1975). However, at fast speeds, the distance covered during flight is much less than for other forms of locomotion (Tucker, 1970; Schmidt-Niesen, 1972, 1984; Thomas, 1975). To meet the high energetic demands of flight, volant animals crafted ingenious strategies in the bioengineering of the organs responsible for energy acquisition and production as well as those directly involved in flight. Bat guts, for example, are modified for high absorptive capacities (Makanya et al. 1997, 2001), and lung volume, pulmonary gas exchange surface areas and pulmonary diffusion capacities are greater than in terrestrial mammals (Maina et al. 1982; Maina & King, 1984; Maina, 2000; Canals et al. 2005a). Indeed, bats have the largest relative heart and lung sizes of all mammals investigated thus far (Canals et al. 2005b). In *Epomophorus wahlbergi*, the subject of the current study, the pulmonary diffusing capacity greatly exceeds that of the shrew, one of the smallest mammals with high metabolic rates (Maina et al. 1982). Though fruit bats may not be some of the highly energetic fliers, *E. wahlbergi* has been reported to travel long distances in search of fruit in one night (Wickler & Seibt, 1976). It is known to make up to three major moves (measuring 500 m to 4 km) per hour while foraging (Fenton et al. 1985). This works out to a range of 36–144 km covered in one night, though the latter figure is most unlikely as only a small percentage of all moves are major, and not all major moves are 4 km (Fenton et al. 1985). This species stands out amongst bats because of its high pulmonary (Maina et al. 1982) and intestinal (Makanya et al. 1997) morphometric values.

The bat wing web is dexterously crafted; the finger bones provide the scaffold distending the patagial membrane, and the abundant blood perfusion proffers an important opportunity for heat dissipation (Kluger &
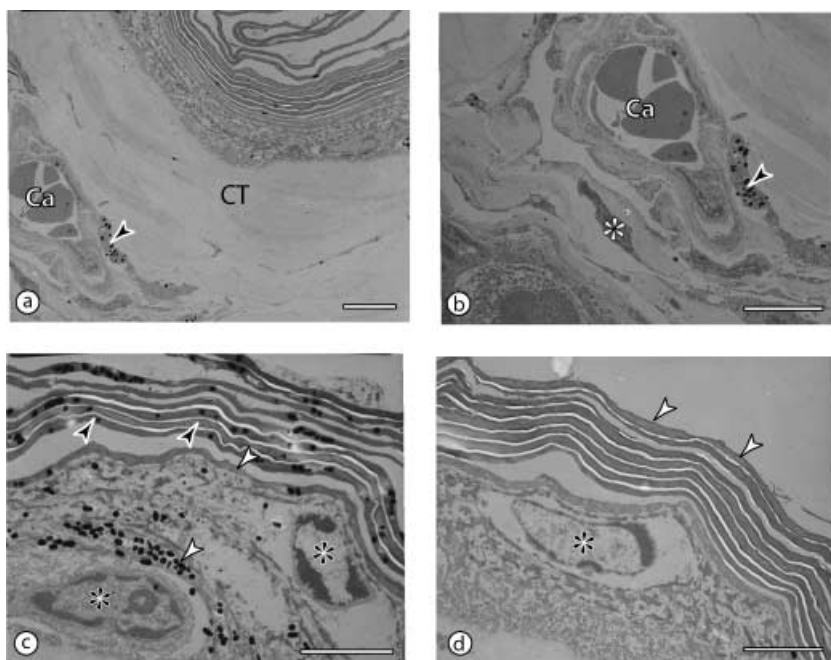

Fig. 5 Transmission electron micrographs of the wing web, showing the layers and the position of the core capillaries. All scale bars = 3 μm. (a,b) The capillaries (Ca) are placed within the core tissue (CT), approximately equidistant from both surfaces. Notice a melanocyte (arrowhead in b) with melanin granules and a fibroblast (asterisk) close to the capillary. (c,d) The non-keratinized part of the epidermis is one to two cells thick (asterisks) and is covered by the stratum corneum with about 10 layers of flattened keratinocytes (dark arrowheads in c; white arrowheads in d). Both the keratinocytes and the other epidermal cells may contain melanin granules (white arrowheads in c).

Fig. 6 Graphs showing $\dot{V}O_2$ (left panel) and $\dot{V}CO_2$ (right panel) of the total body and of the wings, each measured at two temperatures. Unfilled symbols (thin lines) refer to different bats. Filled symbols (thick lines) refer to the mean values of the group, with bars indicating 1 SEM. Note that for clarity, the Y-axis has a different scale below and above the break. At the higher temperature, in most cases total $\dot{V}O_2$ and $\dot{V}CO_2$ decreased, whereas the gas exchange attributed to wings, on average remained almost constant.
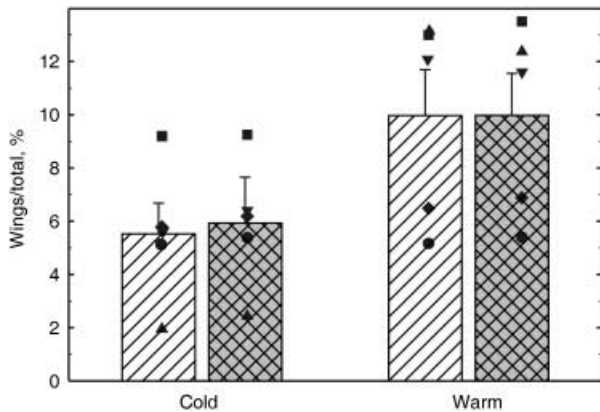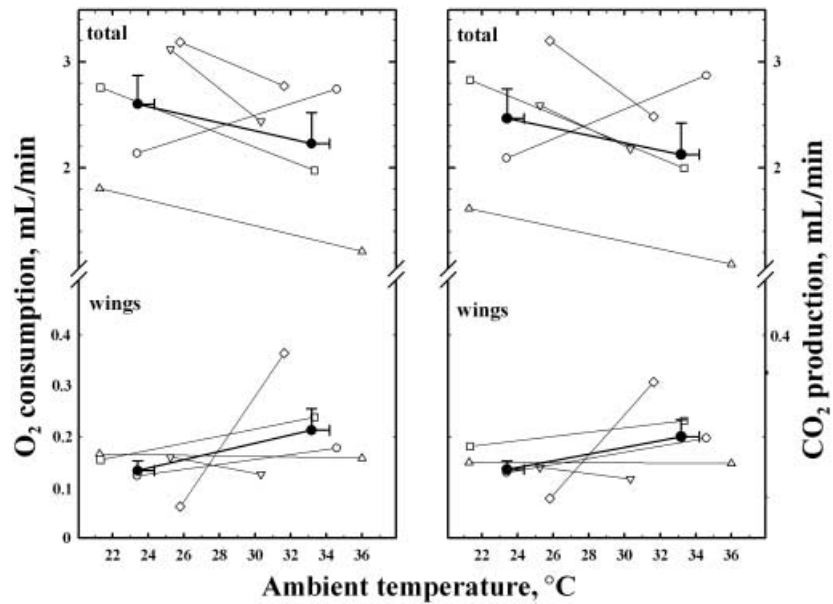

Fig. 7 Gas exchanged through the wings, expressed as percent of the total, during cold and warm conditions. Clear columns refer to measurements of rate of oxygen consumption and filled columns refer to measurements of rate of carbon dioxide production. Columns represent group averages; bars indicate standard errors. Symbols refer to the values of the individual bats.

Heath, 1970; Bakken & Kunz, 1988; Bassett & Studier, 1988; Thompson & Speakman, 1999). The bat wing is fundamentally designed for flight, but it performs many other functions such as thermoregulation, walking and swimming (Jepsen, 1970), food manipulation (Vandoros & Dumont, 2004) as well as trapping of insects (Webster & Griffin, 1962). The large surface area of the wing, the thin skin and the rich blood perfusion combine in providing a measurable contribution to the animal's gas exchange. The result is that in the bat, the skin contribution to the total metabolic needs is the highest ever measured in any adult mammal.

Percutaneous gas exchange is significant in lower vertebrates (Feder & Burggren, 1985), but virtually non-existent in homeotherms, not only due to morphological inadequacy of the skin for gas diffusion, but also because birds

and mammals have high metabolic levels and their surface-to-volume ratios are generally low (MacFarlane et al. 2002). Indeed even in the smallest mammals such as shrews, with a large body surface-to-volume ratio, the skin contributes a maximum of only 3% of total gaseous metabolism (Mover-Lev et al. 1998). The only exceptions are some neonatal marsupials because of their extremely small size and low metabolic requirements (Mortola et al. 1999; MacFarlane & Frappell, 2001). Conversely, in lungless salamanders of the family *Plethodontidae*, percutaneous gas exchange is the primary mode of gas exchange. The lungless European salamander (*Salamandra maculosa*), for example, has a thin epidermis measuring 40–60 μm in thickness with a 5-μm-thick stratum corneum containing 8–12 layers of keratinocytes (Spearman, 1968). This is about four times the thickness of the chiropteran epidermis reported here.

From the allometric equation relating body mass to body surface area, the expected body surface area of a 100-g mammal is 214 cm^2 (Prothero, 1992). In the bat, the surface area of the wing web alone was 3–5 times larger than the expected value. Structurally, the most striking peculiarity of the skin of the wing web is its simple structure; its boneless parts are made up of only an inner layer of connective tissue (Gupta, 1967; Holbrook & Odland, 1978; this study) covered on either side by epidermal cells. The thickness of the wing web subepidermal layer is less than 6% of that in other body regions and, contrary to earlier descriptions of a dermis and hypodermis (Quay, 1970), the boundaries between such strata were equivocal in the current study and no sweat glands or hair follicles were encountered (Figs 3–5). Atmospheric gases therefore have the possibility of reaching the blood vessels from either side, a unique feature for mammalian skin. Elastic fibres within the connective tissue (Holbrook & Odland, 1978) permit the accordion-like folding and unfolding of the

Table 2 Comparison of thickness of selected skin layers in vertebrates that partake of percutaneous gas exchange. All values are in μm

Species	Skin component		
	Epidermis	Stratum corneum	Dermis
European frog (*Rana temporaria*)	80–100	5 (5–6.3)[b]	NR
African clawed frog (*Xenopus laevis*)	16–22	NR	NR
European salamander (*Salamandra maculosa*)	40–60	5 (8–12)[b]	NR
Mexican salamander (*Ambystoma mexicanum*)	70–120	Absent	NR
E. wahlbergi (WWS)	9.1–10.5	3.7–4.4 (41–42)[b]	2.8–8.2[a]
E. wahlbergi (BS)	58–63	17.9–23.3 (31–37)[b]	38.3–52.5

[a]This value represents the combination of dermis and hypodermis as the two layers merge into each other.
[b]The values in brackets in this column represent the thickness of stratum corneum as a percentage of the epidermal thickness. All data were obtained from Spearman (1968) except those for *E. wahlbergi*, which are from the current study.
BS = body skin, WWS = wing web skin, NR = no records.

web membrane, which, with no forces applied to it, rests in a quasi-folded position (Neuweiler, 2000).

The relatively thick stratum corneum (about 40% of the epidermis, Table 2), with multiple layers of squamous keratinocytes, is probably a structural necessity to sustain the continuous air abrasion and shearing stresses during flight, as well as limiting percutaneous water loss. In amphibians, which have an appreciable percentage of cutaneous gas exchange, the stratum corneum takes only 5–12% of the epidermis (Table 2). In the bat wing, the surface–capillary diffusion distance averaged 27 μm, which is less than one third of the thickness of the epidermis in the rest of the body.

An average distance of 27 μm offers an enormous diffusion barrier when compared to the blood–gas barrier of the mammalian lung, which, at places, is as thin as 0.3–0.6 μm (Burri, 1986). However, contrary to the situation in the lung, where the values of partial pressure of O_2 (PO_2) in the alveoli and venous blood are, respectively, about 100 and 46 mm Hg, the capillary blood of the wing skin is exposed to the environmental PO_2 of about 150 mm Hg. Hence, the O_2 pressure gradient for the wing web capillaries is 104 mm Hg (i.e. 150 − 46) or about twice that in the lung, which is 54 mm Hg (i.e. 100 − 46). Functionally, this is equivalent to halving the diffusion distance. This gradient, however, decreases in case of increased humidity, which results in decrease in PO_2 of the ambient air.

In cutaneously respiring lungless salamanders, where about 75% gas exchange occurs through the skin, the thickness of the epidermis alone has been estimated to be between 16 and 100 μm (Spearman, 1968), which is much larger than the 9–10 μm reported here for the fruit bat. In the insectivorous little brown bat, *Myotis lucifugus,* the epidermal thickness has been estimated to range from 30 μm in the distal wing membrane to 90 μm in the exposed areas of nose, lips and sole (Ackert, 1914). Notably, web skin morphology may be variable among bats species, with some having a dorsal, non-vascular layer, and a ventral vascular layer (Jepsen, 1970), whereas others have smooth

muscle cells in their patagial membranes (Kallen, 1977). Unfortunately, investigations on chiropteran wing membrane ultrastructure are scanty and the fine details remain poorly understood.

The chiropteran wing arterioles give rise to several capillaries, in a network of vessels merging into one another. This mesh-type arrangement enlarges the total cross-sectional area of the capillary vascular bed, and keeps the linear velocity of the erythrocytes quite low, as experimentally noticed in '*in vivo*' preparations of the wing web (Davis, 1988a,b). As CO_2 has a high solubility, it diffuses more readily than O_2. Despite this difference in diffusion, $\dot{V}CO_2$ values were seen to be similar to those of $\dot{V}O_2$. This implies that circulation time, rather than diffusion, was the main factor in determining gas transfer in the wing web. Relative to other eutherian mammals, the chiropteran haemoglobin has a higher affinity for O_2 (Boggs et al. 1999) and bats generally have rather low specific metabolic rates, their periods of torpor notwithstanding (Hayssen & Lacy, 1985; Canals et al. 2005a). While the former favours O_2 uptake of the wing web, the low metabolism augments the relative importance of cutaneous gas exchange. The contribution of the wings to total gaseous metabolism increased with the increase in ambient temperatures. In homeotherms, lowering temperature stimulates a thermogenic response, with an increase in $\dot{V}O_2$. This was the case also in the majority of the bats, despite the fact that they were studied under anaesthesia. Presumably, in the bat with the opposite pattern (see unfilled circles in Fig. 6), anaesthesia depressed heat control (Mortola & Gautier, 1995) and the thermogenic response. In such a case, a drop of ambient temperature reduces metabolic rate because of the Q_{10} effect. Conversely, an increase in ambient temperature lowers thermogenesis; hence, the relative contribution of the wings to total gas exchange increases. Furthermore, at high temperatures, the relative contribution of the wings could increase because of the rise in blood perfusion to favour heat dissipation (Kluger & Heath, 1970). This was clearly manifest in only one of the

bats (rhomboid in Fig. 6), but may have been more apparent had we tested the animals without anaesthesia and at higher ambient temperatures.

It is noteworthy that the wing web temperature, especially when the wing is distended, is almost certainly below body temperature. Haemoglobin oxygen affinity increases at lower temperatures, thus favouring oxygen loading in the venous blood. With an increase in ambient temperature, the contribution of the wing could become quite large when the total gas exchange drops. Torpor in bats is characterized by low body temperatures, decline in metabolic rates and apnoeic spells lasting several minutes. Nevertheless, gaseous metabolism has been reported to remain as high as 50% of what was measured during the ventilatory periods (Szewczak & Jackson, 1992). The latter authors interpreted the result as a mixture of gas diffusion and cardiogenic convection within the non-ventilated airways, but in light of what we have found, it seems plausible that cutaneous gas exchange may have been the major contributor.

In addition to the structural and physiological modifications pointed out above, bats have undertaken appropriate behavioural and ecological adaptations to help minimize the metabolic selective pressures. Capacity for flight allows animals to spread far and wide but, unlike birds, which have dispersed widely and even occupied the remote, arid, cold regions of the world (e.g. Antarctica), bats are largely tropical and neotropical in distribution. Only the northern bat (*Eptesicus nilssoni*) is known to exist near the Arctic Circle and has appropriate adaptations to withstand the extreme conditions (Rydel, 1990). Bats therefore, have avoided extreme climatic conditions with poor food resources and their feeding habits are focused on highly nutritious diets (Wimsatt, 1970; Yalden & Morris, 1975). Whether the 6–10% cutaneous contribution to gas exchange described here was an evolutionary adaptation to augment a fundamentally mammalian lung or a contemporary advantage coupled with refinements for heat dissipation remains unclear. Notably, cutaneous gas diffusion occurs without energy expenditure, unlike the pulmonary ventilation, where respiratory muscles are involved.

The large skin surface permeable to gases also predisposes bats to superfluous water loss by evaporation. Cutaneous water loss in chiroptera is considerable (Hattingh, 1972; Laburn & Mitchell, 1975) and may be one reason why the chiropteran diets are based on foods with high water content; indeed, bats also drink water (Bassett & Studier, 1988). The absence of hairs in the wing web skin in the bat greatly facilitates heat dissipation and contemporaneously facilitates gas diffusion. In flying animals, heat dissipation is an essential physiological component as body temperatures often rise to near heat tolerance levels of the somatic tissues (Reeder & Cowles, 1951).

The data in the current study were obtained with bats in resting position, under mild anaesthesia and with folded wings. This implies that much of the wing surface area was not exposed to air, metabolic rates were most likely depressed and air circulation around the wings was hampered. Estimates of the membrane morphometric diffusing capacities of the wing web avail a value of 0.019 ml O_2 min^{-1} mmHg^{-1}, which is about 1% of the total lung diffusing capacity reported by Maina et al. (1982) for this species. The methods used in the latter study overestimate the diffusing capacity of the lung for oxygen (DLO_2) by values as high as 10–20% (Weibel et al. 1993), which means then that DMO_2 would make up a much higher percentage of the DLO_2 than is estimated here. Total diffusing capacity of the wing membrane estimated on adequately stretched wing web membranes and on a larger number of specimens while also taking into account the diffusing capacity of the erythrocytes would result in more elaborate data characterizing the actual diffusing capacity of the patagial membranes. Indeed the epidermal thickness was estimated to be 9.8 μm, and capillaries in the upper regions of the dermis–hypodermis layer would be much closer to the epidermal surface than the diffusion distance of 26.8 μm documented here. Notably, the wing membranes used here were highly folded. Measurement of percutaneous gas exchange during flight would throw more light on the actual contribution of the patagial membranes. Bats and birds are known to increase their $\dot{V}O_2$ from rest to flight by 10- to 20-fold (Thomas, 1987; Butler, 1991).

The wing web has morphological and ultrastructural characteristics that, coupled to numerous functional peculiarities, make some contribution to the animal's total gas exchange. The values for $\dot{V}O_2$ and $\dot{V}CO_2$ reported here are remarkable, noting that they were obtained in anaesthetized bats with folded wings. Higher values would be expected with awake and active bats and especially with wings spread out, as occurs during flight. The functional versatility of the chiropteran wing, however, can only be unraveled by further physiological and structural investigations in diverse species.

Acknowledgements

References

Acharya L (1992) *Epomophorus wahlbergi. Mamm Spec* **394**, 1–4.

Ackert JE (1914) The innervation of the skin of chiroptera. *J Morphol* **25**, 301–343.

Bakken GS, Kunz TH (1988) Microclimate methods. In *Ecological and Behavioural Methods for the Study of Bats* (ed. Kunz TH), pp. 303–332. Washington, DC: Smithsonian Institution Press.

Baker RE (1966) Body composition of the winter and summer *Myotis lucifugus* (Le Conte) (Mammalia: Chiroptera). MS Thesis. Purdue University, Lafayette, Indiana, 79pp.

Bassett JE, Studier EH (1988) Methods of determining water balance in bats. In *Ecological and Behavioural Methods for the Study of Bats* (ed. Kunz TH), pp. 373–386. Washington, DC: Smithsonian Institution Press.

Boggs DF, Maginniss LA, Kilgore DL Jr (1999) In vivo blood oxygen binding in hypoxic lesser sear-nosed bats: relationship to control of breathing. *Respir Physiol* **118**, 193–202.

Burri PH (1986) Development and growth of the human lung. In *Handbook of Physiology, Section 3, The Respiratory System*, Vol. I (eds Fishman AP, Fisher AB), pp. 1–46. Washington, DC: American Physiological Society.

Butler PJ (1991) Exercise in birds. *J Exp Biol* **160**, 233–262.

Canals M, Atala C, Grossi B, Iriarte-Diaz J (2005b) Relative size of hearts and lungs of small bats. *Acta Chiropterol* **7**, 65–72.

Canals M, Atala C, Olivares R, et al. (2005a) Functional and structural optimization of the respiratory system of the bat *Tadarida brasiliensis* (Chiroptera, Molossidae): does airway geometry matter? *J Exp Biol* **208**, 3987–3995.

Carpenter RE (1975) Flight metabolism of flying foxes. In *Swimming and Flying in Nature*, Vol. 2 (eds Wu TYT, Hladik CM), pp. 883–890. New York: Plenum Publishing Co.

Cartlidge P (2000) The epidermal barrier. *Semin Neonatol* **5**, 273–280.

Davis MJ (1988a) Microvascular control of capillary pressure during increases in local arterial and venous pressure. *Am J Physiol* **254**, H772–H784.

Davis MJ (1988b) Control of bat wing capillary pressure and blood flow during reduced perfusion pressure. *Am J Physiol* **255**, H1114–H1129.

Duncker HR (1972) Structure of avian lungs. *Respir Physiol* **14**, 44–63.

Duncker HR, Guentert M (1985) The quantitative design of the avian respiratory system: from humming bird to mute swan. In *Bionareport 3: Bird Flight Vogelflug* (ed. Nachtigall W), pp. 361–378. Stuttgart: Fischer Verlag.

Feder ME, Burggren, WW (1985) Skin-breathing in vertebrates. *Sci Am* **253**, 126–142.

Fenton MB, Brigham RM, Mills AM, Rautenbach IL (1985) The roosting and foraging areas of *Epomophorus wahlbergi* (Pteropodidae) and *Scotophilus viridis* (Verspertilionidae) in Kruger National Park South Africa. *J Mammal* **66**, 461–468.

Frappell P, Lanthier C, Baudinette RV, Mortola JP (1992) Metabolism and ventilation in acute hypoxia: a comparative analysis in small mammalian species. *Am J Physiol* **262**, R1040–R1046.

Gupta BB (1967) The histology and musculature of the plagiopatagium in bats. *Mammalia* **31**, 313–321.

Harris PD, Longnecker DE, Miller FN, Wiegman DL (1976) Sensitivity of small subcutaneous vessels to altered respiratory gases and local pH. *Am J Physiol* **231**, 244–251.

Hattingh J (1972) The correlation between transepidermal water loss and the thickness of epidermal components. *Comp Biochem Physiol A* **43**, 719–722.

Hayssen V, Lacy RC (1985) Basal metabolic rates in mammals: taxonomic differences in the allometry of BMR and body mass. *Comp Biochem Physiol A* **81**, 741–754.

Herreid CF II, Bretz WL, Schmidt-Nielsen K (1968) Cutaneous gas exchange in bats. *Am J Physiol* **215**, 506–508.

Holbrook KA, Odland GF (1978) Collagen and elastic network in the wing of the bat. *J Anat* **126**, 21–36.

Jepsen GL (1970) Bat origins and evolution. In *Biology of Bats*, Vol I (ed. Wimsatt WA), pp. 1–64 Academic Press: New York and London.

Kallen FC (1977) The cardiovascular system of bats: structure and function. In *Biology of Bats*, Vol III (ed. Wimsatt WA), pp. 289–483. New York and London: Academic Press.

Kluger MJ, Heath JE (1970) Vasomotion in the bat wing: a thermoregulatory response to internal heating. *Comp Biochem Physiol* **32**, 219–220.

Laburn HP, Mitchell D (1975) Evaporative cooling as a thermoregulatory mechanism in the fruit bat, *Rousettus aegyptiacus*. *Physiol Zool* **48**, 195–202.

MacFarlane PM, Frappell PB (2001) Convection requirement is established by total metabolic rate in the newborn tammar wallaby. *Respir Physiol* **126**, 221–231.

MacFarlane PM, Frappell PB, Mortola JP (2002) Mechanics of the respiratory system in the newborn tammar wallaby. *J Exp Biol* **205**, 533–538.

Maina JN (2000) What it takes to fly: the structural and functional respiratory refinements in birds and bats. *J Exp Biol* **203**, 3045–3064.

Maina JN, King AS (1984) Correlations between structure and function in the design of the bat lung: a morphometric study. *J Exp Biol* **111**, 43–61.

Maina JN, King AS, King DZ (1982) A morphometric analysis of the lung of a species of bat. *Respir Physiol* **50**, 1–11.

Makanya AN, Maina JN, Mayhew TM, Tschanz SA, Burri PH (1997) A stereological comparison of villous and microvillous surfaces in small intestines of frugivorous and entomophagous bats: species, inter-individual and craniocaudal differences. *J Exp Biol* **200**, 2415–2423.

Makanya AN, Self TJ, Warui CN, Mwangi DK (2001) Gut morphology and morphometry in the epauletted Wahlberg's fruit bat (Epomophorus wahlbergi, Sundevall, 1846). *Acta Biol Hung* **52**, 75–89.

Mortola JP, Frappell P, Woolley PA (1999) Breathing through skin in a newborn mammal. *Nature* **397**, 660.

Mortola JP, Gautier H (1995) Interaction between metabolism and ventilation: effects of respiratory gases and temperature. In *Regulation of Breathing*, 2nd edn. (eds Dempsey JA, Pack AI), pp. 1011–1064. New York: Marcel Dekker.

Mover-Lev H, Minzberg H, Ar A (1998) Is there a significant gas exchange through the skin of the shrew Crocidura russula monacha? *Physiol Zool* **71**:407–13.

Neuweiler G (2000) *The Biology of Bats*, pp. ix, 310. New York: Oxford University Press.

Prothero J (1992) Scaling of bodily proportions in adult terrestrial mammals. *Am J Physiol* **262**, R492–R503.

Pye GW (2001) Marsupial, insectivore, and chiropteran anaesthesia. *Vet Clin N Am Exot Anim Pract* **4**, 211–237.

Quay WB (1970) Integument and derivatives. In *Biology of Bats*, Vol II (ed. Wimsatt WA), pp. 1–56. New York and London: Academic Press.

Reeder WG, Cowles RB (1951) Aspects of thermoregulation in bats. *J Mammal* **32**, 389–403.

Rydel J (1990) The Northern Bat of Sweden: taking advantage of a human environment. *Bats* **8**, 8–11.

Schmidt-Nielsen K (1972) Locomotion: energy cost of swimming, flying and running. *Nature* **177**, 222–227.

Schmidt-Nielsen K (1984) *Scaling: Why Is Animal Size So Important?* Cambridge: Cambridge University Press.

Sears KE, Behringer RR, Rasweiler JJ 4th, Niswander LA (2006) Development of bat flight: morphologic and molecular evolution of bat wing digits. *Proc Natl Acad Sci USA* **103**, 6581–6586.

Spearman RIC (1968) Epidermal keratinization in the salamander and a comparison with other amphibia. *J Morphol* **125**, 129–143.

Szewczak JM, Jackson DC (1992) Apneic oxygen uptake in the torpid bat, *Eptesicus fuscus. J Exp Biol* **173**, 217–227.

Thewissen JGM, Babcock SK (1992) The origin of flight in bats. *BioScience* **42**, 340–345.

Thomas DW (1975) Metabolism during flight in two species of bat: *Phyllostomus hastatus* and *Pteropus gouldii. J Exp Biol* **57**, 317–335.

Thomas SP (1987) The physiology of bat flight. In *Recent Advances in the Study of Bats* (eds Fenton MB, Racey P, Rayner JMV), pp. 75–99. Cambridge: Cambridge University Press.

Thomspon SC, Speakman JR (1999) Absorption of visible spectrum radiation by the wing membranes of living pteropodid bats. *J Comp Physiol B* **169**, 187–194.

Tucker VA (1970) Energetic cost of locomotion in mammals. *Comp Biochem Physiol Physiol* **14**, 75–82.

Vandoros JD, Dumont ER (2004) Use of the wings in manipulative and suspensory behaviors during feeding by frugivorous bats. *J Exp Zool* **301A**, 361–366.

Webster FA, Griffin DR (1962) The role of flight membranes in insect capture by bats. *Anim Behav* **10**, 332–340.

Weibel ER, Federspiel WJ, Fryder-Doffey F, Hsia CC, Konig M, Stalder-Navarro V, et al. (1993) Morphometric model for pulmonary diffusing capacity. I. Membrane diffusing capacity. *Respir Physiol* **93**, 125–149.

Wickler W, Seibt U (1976) Field studies of the African fruit bat *Epomophorus wahlbergi* (Sundeval), with special reference to male calling. *Z Tierpsychol.* **26**, 726–736.

Wiegman DL, Harris PD, Longnecker DE, Miller FN (1975) Microvascular response to hypoxia, hyperoxia, hypercarbia and localized acidosis. *Bibl Anat* **13**, 159–160.

Wimsatt WA (1970) *Biology of Bats.* London: Academic Press.

Yalden DW, Morris PA (1975) *The Lives of Bats.* New York: The New York Times Book Co.